Diagnosis of Fault On 330kV Power System Transmission Lines Using Artificial Neural Network and Travelling Wave.

KAZAKA T. D.[1], OGBOH V. C.[2], OBUTE K. C.[3], OYIOGU D. C[4]

[1, 2, 3, 4]Department of Electrical Engineering, Faculty of Engineering, Nnamdi Azikiwe University, Awka

Abstract- The reliability and stability of high-voltage power transmission systems are critical for efficient energy delivery and national grid integrity. In this study, we investigate the application of Artificial Intelligence (AI) techniques for the diagnosis of faults on 330kV power system transmission lines. Traditional fault detection and location methods often suffer from latency, reduced accuracy under complex fault conditions, and limitations in real-time analysis. This research leverages machine learning algorithms, including Artificial Neural Networks (ANN), Support Vector Machines (SVM), and Decision Trees (DT), to detect, classify, and locate various types of faults—such as single line-to-ground (SLG), line-to-line (LL), double line-to-ground (DLG), and three-phase faults—based on real-time voltage and current signal features. Simulations were conducted using MATLAB/Simulink to model the transmission network and generate training datasets under diverse operating conditions. The AI models demonstrated high accuracy and robustness in fault classification and location estimation, with significantly improved speed compared to conventional methods. This work highlights the potential of AI-driven systems to enhance fault management in high-voltage transmission networks, reduce downtime, and support proactive maintenance strategies in smart grid applications. Let me know if you want it tailored toward a specific region or case study (like Nigeria or a particular substation), or if you want to add performance metrics or specific AI models.

Indexed Terms- Transmission Line, Artificial Neural Network, Fault, Traveling Wave, Location.

I. INTRODUCTION

The problem of detecting transmission line faults is as old as the power industry itself. In the beginning, the fault detection was by direct visual inspections of the line. However, the visual inspection of a long line, foot or by air, is always extremely slow and subject to the terrain circumstances and environmental conditions of the moment. Additionally, visual inspection does not always ensure that the location is found because in many cases, faults do not leave physical evidence.

Considering the rapid growth in the power grid network over the past decades all over the world which eventually led to the installation of a large number of new transmission and distribution lines, the deregulation of electric power has increased the need for reliable and uninterrupted electric power supply to the end users who are very sensitive to power outage. One of the biggest problems in the electrical power system is the interruption or discontinuity of power supply, which is caused by the occurrence of faults.

Faults in transmission lines refer to any abnormal condition that disrupts the normal operation of the line, causing outages, equipment damage, or reduced transmission efficiency. Faults occur when two or more conductors make contact with one another or with ground in a three-phase system, which can either be a symmetrical fault or an unsymmetrical fault. These faults cause grave damage to power system components; it is not only the equipment that is affected by the faults, but the power quality also gets poor. Therefore, in order to prevent the power system equipment from damage and to enhance the power quality, it becomes imperative to diagnose the type of fault and its location on the transmission line so that it can be removed with suitable means (protective devices such as relays and circuit breakers). The faults are usually taken care of by devices that detect the occurrence of a fault and eventually isolate the faulted section from the rest of the power system.

As a result, some of the important challenges for the incessant supply of power are detection, classification,

and location of faults (Saha et al, 2006). Most of the research done in the field of protective relaying of power systems concentrates on transmission line fault protection because transmission lines are relatively very long and can run through various geographical terrain and hence it can take from a few minutes to several hours to physically check the line for faults (Eriksson et al, 2015).

Hence, many utilities are implementing fault locating devices in their power quality monitoring systems that are equipped with Global Information Systems for easy location of these faults. Fault location techniques can be broadly classified into the following categories (Saha et al, 2010):

II.   METHODOLOGY

This chapter presents the methodological procedure for the implementation of the aim and objectives of this research. Given in Figures 1.0 and 3.3 is a flowchart diagram that represents the methodological procedure for this research.
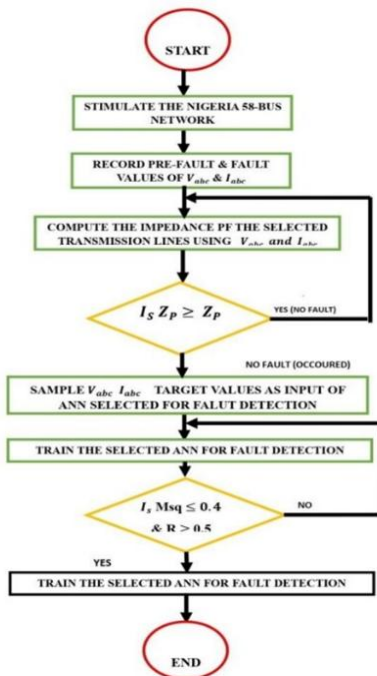

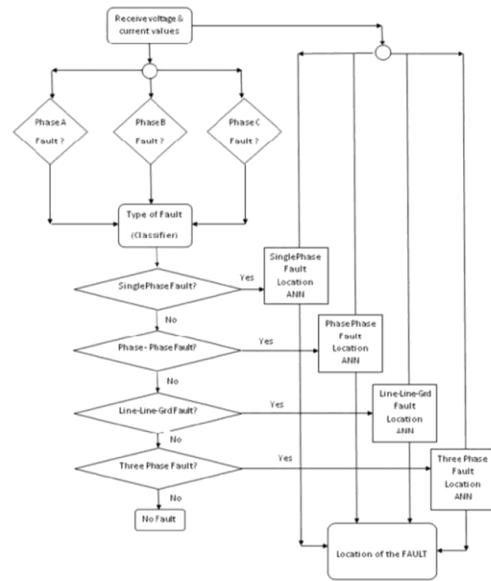Figure 1: Flowchart of the research methodology

Figure 2: Flowchart showing the outline of the ANN

At the decision box in Figure 3.1, if the relay set impedance Zp is greater than or equal to the fault impedance on the line Zf, no fault on the line, there will be no further operation, but if the impedance Zp is less than the fault impedance Zf, the fault is detected.

Modeling of the Nigerian 58–Bus Network
The Nigerian 58–Bus Power System Network is built using the following parameters in Tables 3.1 and 3.2. Also, the 58–Bus Network is modeled using the Matlab/Simulink tool for the implementation of the ANN selected structure for the detection of faults on the Power System Network.

Artificial Intelligence (AI) combines neural networks, signal processing, and mathematical modeling to analyze faults on a 330 kV power transmission line. A thorough procedure for carrying out this analysis is provided below;

A Mathematical Modeling of the Transmission Line
When a 330 kV transmission line is mathematically modeled, its electrical properties and behavior under different circumstances are represented. This detailed explanation will include:
• Transmission Line Parameters
• Transmission Line Modeling Approaches
• Derivation of Equations
• Numerical Calculation Example
• Equivalent Circuit Representations

B. The Transmission Line Parameter

Transmission line parameters include:
- Resistance (R), Inductance (L), Capacitance (C): Represent line characteristics.
- Distributed Model: A 330 kV line is long, so distributed parameters are preferred over lumped parameters.

Voltage (V(x,t)) and current (I(x,t)) are governed by the Telegrapher's equations below:

$$\frac{\partial V}{\partial x} = -RI - L\frac{\partial I}{\partial t} \tag{1.0}$$

$$\frac{\partial I}{\partial x} = -GV - C\frac{\partial V}{\partial t} \tag{2.0}$$

Where G is the conductance.
Conductor Resistance (R): This represents the losses due to the flow of current through the conductor, as shown in equation 3.0.

$$R = \frac{\rho}{A} \tag{3.0}$$

Where ρ is the resistivity of the aluminum conductor material with a value $2.82 \times 10^{-8} \Omega.m$
A is the cross-sectional area of the aluminum conductor.
Inductance (L): This parameter includes both self-inductance and mutual inductance, which is given in equation 4.0.

$$L = 2 \times 10^{-7} \ln\ln\left(\frac{D_m}{r^I}\right) H/m \tag{4.0}$$

where:
D_m is the Geometric mean distance (GMD) between the conductor and r^I is the effective radius of the conductor, including skin effect.
Capacitance (C): This is the electric field between the conductors and the ground given in equation 5.0.

$$C = \frac{2\pi\epsilon_0}{ln\left(\frac{D_m}{r}\right)} F/m \tag{5.0}$$

Where ϵ_0 is 8.854 x 10^{-12}F/m and r is the actual radius of the conductor.
Conductance(G):
Represents leakage current due to imperfect insulation and environmental conditions. Usually very small and often neglected.

C. Transmission Line Modeling Approaches
The 330 kV line is categorized as a long transmission line (length >250 km). Its behavior is best described using a distributed parameter model.

D. Distributed Parameter Model
The transmission line is modeled by the Telegrapher's Equations:

$$\frac{\partial V}{\partial x} = -(R + j\omega L)I \tag{6.0}$$

$$\frac{\partial I}{\partial x} = -(G + j\omega C)V \tag{7.0}$$

Where V(x, t) is the voltage along the line, I(x,t) is the current along the line, and $\omega = 2\pi f$ is called the angular frequency of the system (50Hz).

Solution of the Telegrapher's equations
The voltage and current can be expressed as traveling waves in equations 8.0 and 9.0.

$$V(x) = V_+ e^{-\gamma x} + V_- e^{\gamma x} \tag{8.0}$$

$$I(x) = \frac{1}{Z_C}(V_+ e^{-\gamma x} + V_- e^{\gamma x}) \tag{9.0}$$

Where,

$$\gamma = \sqrt{(R + j\omega L)(G + j\omega C)} \quad \text{called propagation constant} \tag{10.0}$$

$$Z = \sqrt{\frac{(R+j\omega L)}{(G+j\omega C)}} \text{ called characteristic impedance (11.0)}$$

E. Numerical Calculation of Transmission Line Data
Line Length = 96Km
Conductor Resistance R = 0.02Ω/Km
Inductance L= 1.2mH/Km
Capacitance C = $0.01 \mu f / Km$
Conductance G = (Negligible) S/Km
Step 1:
Calculation of the Propagation constant (γ)

$$\gamma = \sqrt{(R + j\omega L)(G + j\omega C)}$$

R = 0.02, L = 1.2 x 10-3, G = 0, C = 0.01 x 10-6, $\omega = 2\pi \times 50 Hz$

$$\gamma = \sqrt{(R + j\omega L)(G + j\omega C)} =$$
$$\sqrt{(0.02 + j(2 \times 3.142 \times 50 \times 1.2 \times 10^{-3})(j(2 \times 3.142 \times 50 \times 0.01 \times 10^{-6}))} =$$
$$\sqrt{0.02 x j(1.13112)(j(0.030143)} = 0.1414\Omega \tag{12.0}$$

Calculation of the Characteristic Impedance (Z_c)

$$(Z_c) = \sqrt{\frac{(R+j\omega L)}{(G+j\omega C)}} = \sqrt{\frac{(0.02+j(2 \times 3.142 \times 50 \times 1.2 \times 10^{-3})}{(j(2 \times 3.142 \times 50 \times 0.01 \times 10^{-6})}} = j338.49\Omega \tag{13.0}$$

F. Fault Analysis
Equation 3.14 can be used to model faults on the line by determining the fault current for each fault situation;

$$I_f = \frac{V}{Z_{total}} = \frac{V}{Z_{source} + Z_{line} + Z_f} \tag{14.0}$$

Where;
Z_{source} is the source impedance
Z_{line} is the line impedance
Z_f is the fault impedance
I_f is it the fault current?
This mathematical framework models a 330 kV transmission line in a comprehensive way by combining numerical techniques, steady-state analysis, and transient behavior.

In many practical applications, the negative and positive sequence impedances are found to be equal. If

the generator is solidly grounded, $Z_n = 0$, and for a bolted fault, $Z_f = 0$.

It should be noted that the three-phase balanced source impedance is zero (0), since the synchronous generator with neutral is grounded through an impedance Z_n. Saadat, H. (1997).

G. Fault Conditions
Equation 3.14 is used for a mathematical study of fault conditions.

Three-phase, line-to-line (LL), double-line-to-ground (DLG), and single-line-to-ground (SLG) faults can all be simulated.

In a 330 kV power system transmission line, fault circumstances entail figuring out fault currents, fault voltages, and the consequences of various fault kinds. These comprise three-phase faults, line-to-line (LL), double-line-to-ground (DLG), and single-line-to-ground (SLG) faults. Nilesh and Singh (2016). Symmetrical components are used in fault analysis to make computations easier.

3.2.4 Symmetrical Components Basics
Voltage and Current Decomposition
Voltage Va, Vb, Vc and Ia, Ib, Ic are expressed in terms of symmetrical components:

$$\begin{bmatrix} V_a \\ V_b \\ V_c \end{bmatrix} = \begin{bmatrix} 1 & 1 & 1 \\ 1 & a & a^2 \\ 1 & a^2 & a \end{bmatrix} \begin{bmatrix} V_0 \\ V_1 \\ V_2 \end{bmatrix}$$
(15.0)

$$\begin{bmatrix} I_a \\ I_b \\ I_c \end{bmatrix} = \begin{bmatrix} 1 & 1 & 1 \\ 1 & a & a^2 \\ 1 & a^2 & a \end{bmatrix} \begin{bmatrix} I_0 \\ I_1 \\ I_2 \end{bmatrix}$$
(16.0)

$$a = e^{j120^0} = -\frac{1}{2} + j\frac{\sqrt{3}}{2}$$
(17.0)

V_0, V_1, V_2 are zero, positive, and negative sequence voltages. This happens under a fault condition.
I_0, I_1, I_2 are zero, positive, and negative sequence currents.

H. Fault Types and Analysis
I. Single-Line-to-Ground Fault (SLG)
Fault occurs on phase a (e.g. Va = 0)
Boundary conditions: $V_a = 0$, $I_b = 0$, $I_c = 0$
Therefore,
Relationship among symmetrical components:
$V_0 + V_1 + V_2 = 0$ (3.18)
$I_0 = I_1 = I_2 = I_a$ (3.19)
Sequence network connection: Zero, positive, and negative sequence networks are connected in series.
Fault Current:

$$I_f = \frac{3V_1}{Z_0 + Z_1 + Z_2 + z_f}$$
(3.18)

Where,
Z_0, Z_1, Z_2 are zero, positive and negative sequence impedance of the line.
Z_f is the fault impedance,
V_1 is the pre-fault positive-sequence voltage at the fault point.

II.   Line-to-Line Fault (LL)
Fault occurs between phases b and c   (e.g.)
Vb = Vc) (19)
Boundary conditions Vb = Vc, Ia = 0   (20)
Relationship among symmetrical components
$V_2 = -V_1$, $V_0 = 0$ (21)
$I_2 = -I_1$, $I_0 = 0$ (22)
Sequence network connection: Zero, positive, and negative sequence networks are connected in series.
Fault current is given by;

$$I_f = \frac{3V_1}{Z_0 + Z_1 + Z_2 + 3Z_f}$$
(23)

III.   Double-Line-to-Ground   Fault (DLG)
The fault occurs between phases b and c and the ground.
Boundary conditions Vb = Vc, Va = 0   (20)
Relationship among symmetrical components
$V_0 = V_1 = V_2$ (21)
$I_0 + I_1 + I_2 = 0$ (22)
Sequence network connection: Zero, positive, and negative sequence networks are connected in series.
Fault current is given by;

$$I_f = \frac{3V_1}{Z_1 + Z_2 \| (Z_0 + Z_f)}$$
(23)

IV.   Three-Phase Fault
The fault occurs between phases b and c and the ground.
Boundary conditions Vb = Vc, Va = 0   (24)
Relationship among symmetrical components
$V_0 = V_2 = 0$, $V_1 = V_2$ (25)
$I_0 + I_1 + I_2 = 0$ (26)
Sequence network connection: Zero, positive, and negative sequence networks are connected in series.
Fault current is given by;

$$I_f = \frac{V_1}{Z_1 + Z_f}$$
(27)

Fault Current Calculation
Given Data:
$Z_I = 0.1 + j0.5\Omega$ (28)
$Z_2 = 0.1 + j0.5\Omega$ (29)
$Z_0 = 0.3 + j1.0\Omega$ (30)
$Z_f = 0\Omega$ (for bolted fault)
Pre-fault voltage $V_1 = \frac{330kV}{\sqrt{3}} = 190.5Kv$ (31)

SL - G Fault

$$I_f = \frac{3V_1}{Z_{total}} = \frac{3V_1}{Z_0 + Z_1 + Z_2 + 3Z_f} \qquad (32)$$

Substitute:

$$I_f = \frac{3 X 190.5}{(0.3+j1.0)+(0.1+j0.5)+(0.1+j0.5)+3(0)} = \frac{571.5}{0.5+j2.0} =$$

$$\frac{571.5}{2.06\angle 75.96^0} = 277.2\angle -75.96^0 \; kA \qquad (33)$$

L - L Fault

$$I_f = \frac{\sqrt{3}V_1}{Z_1 + Z_2 + Z_f} \qquad (34)$$

$$I_f = \frac{\sqrt{3} X 190.5}{(0.1+j0.5)+(0.1+j0.5)} = \frac{329.96}{0.2+j1.0} = \frac{329.96}{1.02\angle 78.69^0} =$$

$$323.55\angle -78.69^0 \; kA \qquad (35)$$

L – L - L Fault

$$I_f = \frac{V_1}{Z_1 + Z_f} \qquad (36)$$

$$I_f = \frac{190.5}{(0.3+j1.0)+(0)} = 182.5\angle -73.30^0 \; kA \qquad (37)$$

J.   Modeling of the Nigerian 58 – Bus Network

The parameters in Tables 3.1 and 3.2 are used to build the Nigerian 58-Bus Power System Network.

The MATLAB/Simulink tool is used in modeling the 58-Bus Network so as to apply the ANN-selected structure for the Power System Network defect identification.

Table 1: Classification and Representation of Transmission Lines

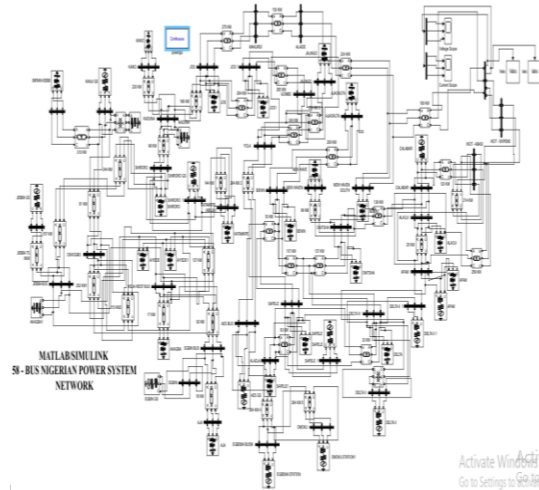| S/NO	TYPE OF LINE	LINE LENGTH (Km)	MODEL OF REPRESENTATION	REMARKS
1	Short Line	Up to 80 (50miles)	Series Impedance (R + jX_L)	Neglects Shunt X_C
2	Medium Line	80 to 240 (50 to 150 miles)	Normal π or T network	Lumped Parameters
3	Long Line	Above 240 (Above 150 miles)	Equivalent π or T network	Distributed Parameters

https://://www.site.Outtawa.ca.
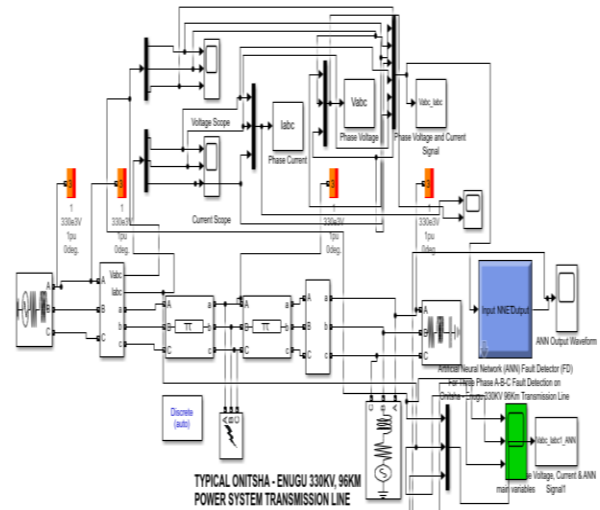

Figure 3: Nigeria 58-Bus Power System Network

Figure 4: A MATLAB/Simulink Model of Onitsha – Enugu of Nigeria 58 – Bus Power System Network

The network is made up of Generating Stations, -Transmission Lines, -Buses, and -Loads.

Taking the 330KV transmission line between Onitsha and Enugu, which is 96 kilometers away, as our case study area. It falls under the medium line category and since it corresponds to a line length of more than 80 kilometers.

The transmission line's shunt reactance (Jωcl), also known as its shunt admittance, is so little that it is insignificant, leading to the simple equivalent circuit shown in Figure 3.5.
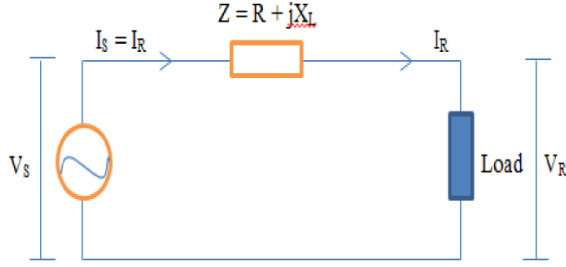
Figure 5. Equivalent Circuit of Medium Transmission Line

The voltage and current relationship between the sending and receiving ends is given in the equations below;

$$[V_S I_S] = [1Z01][V_R I_R] \tag{38}$$

Thus,

$$|V_S| = [(|V_R|cos\emptyset_R + |I|R)^2 + (|V_R|sin\emptyset_R + |I|X_L)^2]^{\frac{1}{2}} \tag{39}$$

$$|V_S| = [(|V_R|^2 + |I|^2(R + X_L)^2 + 2(|V_R||I|(Rcos\emptyset_R + X_L sin\emptyset_R)]^{\frac{1}{2}} \tag{40}$$

$$|V_S| = |V_R|[1 + \frac{2|I|Rcos\emptyset_R}{|V_R|} + \frac{2|I|X_L sin\emptyset_R}{|V_R|} + \frac{2|I|^2 X_L(R^2 + X_L^2)}{|V_R|^2}]^{\frac{1}{2}} \tag{41}$$

$$\frac{2|I|^2 X_L(R^2 + X_L^2)}{|V_R|^2} \cong 0$$

Then,

$$|V_S| = |V_R|[1 + \frac{2|I|Rcos\emptyset_R}{|V_R|} + \frac{2|I|X_L sin\emptyset_R}{|V_R|}]^{\frac{1}{2}} \tag{42}$$

Nevertheless, using binomial expansion while keeping first-order terms, gives; $|V_S| = |V_R|[1 + \frac{2|I|Rcos\emptyset_R}{|V_R|} + \frac{2|I|X_L sin\emptyset_R}{|V_R|}]^{\frac{1}{2}} \tag{43}$

$$|V_S| = |V_R| + |I|(Rcos\emptyset_R + X_L sin\emptyset_R) \tag{44}$$

K. Artificial Neural Network Application

$$h_j^H = b_j + \sum_{T=1}^{NI} W_{ji} X_1 \tag{47}$$

Each neuron of the hidden layer takes its input h_j^H and uses it as the argument function and produces an output given by

$$y_j^H = \emptyset \, h_j^H \tag{48}$$

Then, the inputs to the neurons of the outputs layer are calculated as

$$h_k^o = b_k + \sum_{j=1}^{NH} W_{kj} y_j^H \tag{49}$$

However, the network output is then given by;

$$y_k = \emptyset \, (h)_k^o \tag{50}$$

L. The Error Back-Propagation Learning Algorithm

An output error is the difference between the network output and the desired output value, or for the Kth output neuron.

The output error of the Kth output neuron is given as

$$e_k = d_k - y_k \tag{51}$$

d_k = desired output value

y_k = Network output value

The summed square errors can be found using the output error in the manner described below:

$$\varepsilon = \frac{1}{2}\sum_{k=1}^{NO} e_k^2 \tag{52}$$

Reducing this error is the aim of the learning process. It depends on every network variable, and we can determine the gradient of the error to the weight matrix that connects the hidden layers to the output layer using the chain rule as shown below;

$$\frac{\partial \varepsilon}{\partial w_{kj}} = (\frac{\partial \varepsilon}{\partial e_k})(\frac{\partial e_k}{\partial y_k})(\frac{\partial y_k}{\partial h_{ko}})(\frac{\partial h_{ko}}{\partial w_{kj}}) \tag{53}$$

If we compute each term, we will obtain as follows:

$$\frac{\partial \varepsilon}{\partial w_{kj}} = e_k \tag{54}$$

$$\frac{\partial e_k}{\partial y_k} - 1 \tag{55}$$

$$\frac{\partial y_k}{\partial h_{ko}} = \emptyset_k \, hko \tag{56}$$

$$\frac{\partial h_{ko}}{\partial w_{kj}} = y_j^H \tag{57}$$

But, if we combine these expressions above, we will obtain that;

$$\frac{\partial \varepsilon}{\partial w_{kj}} = e_k \emptyset_k (hko) y_j^H \tag{58}$$

The change ▲wkj, which is applied to the weight matrix that is connected to the hidden layer to the output layer, is also given as

$$\Delta W_{kj} = -\eta \frac{\partial \varepsilon}{\partial w_{kj}} = -\eta e_k \emptyset_k h_k^O y_j^H \tag{59}$$

Where ŋ is a constant known as the step size or learning rate. We can also rewrite the equation (58) as:

$$\Delta W_{kj} = -\eta \delta_k y_k^H \tag{60}$$

Where $\delta_k = e_k \emptyset_k(hko)$ is called the local gradient term. However, in accordance with the following equation, we must repeat the above process in order to update the weights that link the input layer to the hidden layer.

But to update the weights connecting the input layer to the hidden layer, we need to repeat the procedure above according to the following equation.

$$\frac{\partial \varepsilon}{\partial w_{kj}} = (\frac{\partial \varepsilon}{\partial e_k})(\frac{\partial e_k}{\partial y_k})(\frac{\partial y_k}{\partial h_{ko}})(\frac{\partial h_{ko}}{\partial w_{kj}})(\frac{\partial y_j^H}{\partial h_j^H})(\frac{\partial h_j^H}{\partial w_{ji}}) \tag{61}$$

Following the computation of the aforementioned terms, the relationship to the weight matrix is expressed as follows:

$$\Delta W_{ij} = -\eta \delta_j X_i \tag{62}$$

$$\delta_j = \emptyset_j(h_j^H) \sum_{k=1}^{NO} \delta_k W_{kj} \tag{63}$$

Therefore, in general, the connection term is calculated using:

$\Delta W_{im} = \eta \delta_m X_i$ = Learning rate x local gradient Input to the layer (64)

The Neuron Transfer Function: The neuron transfer functions Ø (.) of the hidden layer are different from the ones in the output layer. These activation or transfer functions come in a variety of forms and are employed to generate an output and choose the appropriate weighted input sum.

The neuron's task determines which transfer function is used. Different types of transfer functions that are frequently employed in neural networks are depicted in equations (65) and (66).

The hard limit A transfer function of this type sets the neuron's output to zero if the net input value n is less than zero or to one if n is larger than or equal to zero.

The linear transfer function: After multiplying the neuron's signal by a gradient constant (slope), this function adds a neuron bias to the output.

The log-sigmoid transfer function: In back propagation networks, the log-sigmoid transfer function is frequently employed. It is employed to generate an output that fluctuates between 0 and + I while the input fluctuates between - and ∞. According to Ogboh (2019), it is a differentiable function.

The output layer typically uses the linear transfer function, whereas the hidden layer often uses the sigmoid function.

The log–sigmoid transfer function is defined as;
$$Y = \frac{(1)}{(1+e-x)} \quad -\infty < x < \infty \qquad (65)$$
Since the log-sigmoid function is differentiable, Therefore,
$$\frac{\partial y}{\partial x} = \frac{e-x}{(1+e-x)^2} = Y(1-Y) \qquad (66)$$

3.5 Detection of Faults using Artificial Neural Network (ANN)

The methodological process for developing ANN for defect detection is presented in this section. The three stages of the ANN used here are isolation, classification, and detection. An ANN is chosen and trained for its task at each step.

The inputs of each network are the three-phase currents (I = {IaIbIc}T) and voltages (V = {Va VbVc}T) of the line generated using the Power system block set (simpowersystem).

These three goals should be achieved via a thorough fault diagnosis plan for transmission line systems. Nasim (2018)

1. Fault Detection: The purpose of fault detection is to determine whether or not a transmission line fault has occurred.
2. Fault classification: Here, the types of faults are determined.
3. Fault location: The purpose of fault location is to identify the zone in which the faulty line is situated.

i. Selecting the proper network

The best and most acceptable function approximates are multilayer perceptual networks, while the best algorithm for training a network for function approximation is supervised learning. Additionally, for generalization, a back-propagation learning method is employed; however, it necessitates a lengthy training period and may only cover a small amount of data.

ii. Training of the Selected ANN

One of the most crucial stages in the creation of ANN detectors and locators is training neural networks; hence, training data needs to be carefully and methodically prepared. A training simulator can be used to generate pertinent data for ANN training in situations when training data is not always available as part of a real system.

It is important to create training data that is representative of all potential situations in which the ANN may be used to carry out its detection and classification tasks. As a result, training data can grow into enormous data sets. For training, the back-propagation algorithm (BPNN) has been employed. Figure 3.11gives an overview of the training process. The training data employed in this work include;

• Pre-fault (No Fault) Condition:

The training data used for No fault condition are the pre-fault voltage and current magnitude signal in per unit.

Training the ANN network on No fault will give pre-fault voltage and current waveform that shows that the voltage magnitudes are far greater than the current magnitudes since there are no faults in the system. The ANN network architecture is then connected to the system, which will make use of the pre-fault voltage and current (V & I) as six inputs of the ANN, which will produce the ANN response for pre-fault condition (i.e No fault)

• Fault Condition:

The training data used for fault condition are the fault voltage and current magnitude signal in per unit.At three phase fault for fault detection, the three phase fault voltage and current signal per unit values are used as six inputs to the ANN network. These when trained will produce three phase fault voltage, current and ANN response, that shows voltage has dropped to

approximately 0pu while the current increases, showing that fault has occurred.

Each layer of neurons in the artificial neural network (ANN) serves as an input to the layers that follow. Weights are used to regulate each layer, which strengthens the signal transmission. The output generated by the traditional approach is an actual output, while the output generated by BPNN is a target output.

We can better grasp the discrepancy (error) between the intended and actual process outputs by utilizing the error to determine the Least Mean Square Error. The BPNN propagates errors backwards from the output layer when a null error is obtained. Tayeb (2014).

Figures 9 and 10 also show a selection and sampling process for the input data of the ANN.
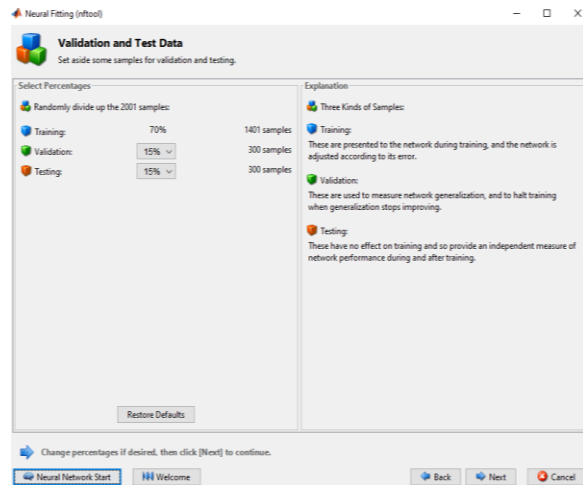
Figure 9: Selection and Sampling of Input Data into ANN

The validation and test data is a training process that displays the precise number of input data samples (Vabc_Iabc) data extracted for training, validation, and testing of the ANN. It shows that a total of 1401 samples (70% of 2001) and 300 samples (15% of 2001) were utilized for training, validation, and testing, respectively.
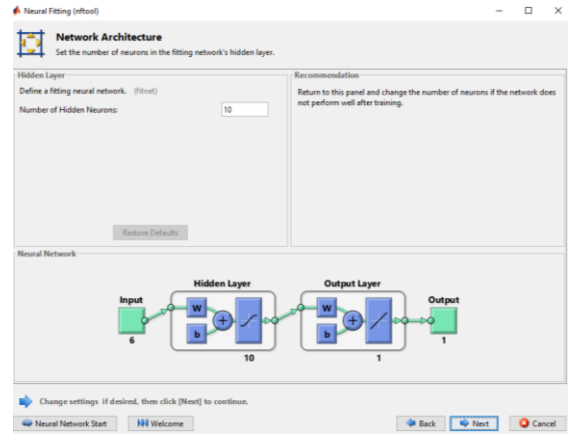
Figure 10: Selection and Sampling of Input Data into ANN

The chosen ANN network architecture for defect detection and training is displayed in Figure 10. This ANN structure helps us to choose intelligently the number of neurons in the hidden layer of the architecture.

The training network window, trains the chosen network and samples using the Levenberg-Marquardt backpropagation training algorithm. If regression and mean square error values are not reached, retraining may be necessary. Until a convergence (Mean Square ≤ 0.4 and Regression R $\leq 1 \geq 0.5$) is achieved, the retraining and neuronal count change will continue.

Electrical problems serve as the foundation for this investigation, and the ANN Fault Detector is trained with a variety of reasons for matching to various types of data. Through simulation, the trained ANN is validated, and both the performance and accuracy of the outputs are confirmed. As a result, evaluating and validating ANN output to input data is crucial.

An ANN must be constructed by explaining and correlating the neural network's inputs and outputs in order to recognize patterns. It is important to carefully analyze the inputs to the network, which provide a picture of the state and transient characteristics of the defects to be identified.

The neural detector's function is to identify whether a transmission line fault is present or absent. By immediately determining the power system state, beginning with the instantaneous voltages and currents, the appearance of such a defect is determined. As a result, a scaling strategy (also known as signal normalization) is crucial for cutting down on the execution computing time before the voltage and current data enter the neural network. We used a scaling method for this, which is represented by

dividing the fundamental voltage and current magnitudes.

An artificial neural network (ANN) is a flexible system that can generalize to new, unseen data and learn associations through repeated data presentation. This is accomplished through training, which is predicated on learning.

M. Mathematical Approach for Fault Location Impedance-Based Method

$$Z_f = \frac{V_f}{I_f} \tag{67}$$

$$d = \frac{Z_f}{Z_{line}} \ X \ \text{L}_{line} \tag{68}$$

Where Z_f is the fault impedance, Z_{line} is the line impedance, and L_{line} is the total line length and d is the distance.

N. Traveling Wave Method

The traveling wave method was engaged to locate faults on the case study 330Kv power system transmission line. Using the wavefront arrival times (t_1, t_2), equation 3.69 given below was used to identify line faults.

$$d = \frac{v}{2} \ x \ (t_2 - t_1) \tag{69}$$

Where, d is the located fault distance, t_1 and t_2 are wavefront arrival times.

A voltage wave that travels from the supply source end to the far end may be responsible for the line voltage's steady development. The line capacitances' progressive charging will account for the associated current wave. Assume that in a very short amount of time t, a current I and a voltage V are established over a line length x. The emf V is balanced by the back emf generated by the magnetic flux generated by the current in this line length. The flux built up is ILδx, and the back emf is the rate of buildup, thus; IL δx/δt, since the inductance of the length δx is Lδx (L is line inductance per unit length) (Ogboh et al, 2019).

So we have

$$V = IL\frac{\delta x}{\delta t} = ILv \tag{70}$$

Where v is the velocity of propagation of wave.
During time δt, the current I carries a charge Iδt, which stays on the line to charge it to the potential of V. Since the line's charge is VCδx and its capacitance of length δx is Cδx (where C is the line's capacitance per unit length), so we have;

$$I\delta t = VC\delta x \tag{71}$$

or

$$I = VC\frac{\delta x}{\delta t} = VCv \tag{72}$$

The switching of an emf V on to the line results, therefore in a wave of current I and velocity v are given by equations (70) and (72). Dividing equation (3.70) by equation (72), we have;

$$\frac{V}{I} = \frac{ILv}{VCv} = \frac{I}{V} \cdot \frac{L}{C} \tag{73}$$

or

$$\frac{V^2}{I^2} = \frac{L}{C} \tag{74}$$

or

$$\frac{V}{I} = \sqrt{\frac{L}{C}} = Z_n \tag{75}$$

This formula is known as the line's surge impedance since it is a ratio of voltage V to current I, which has impedance dimensions. Because this impedance solely depends on the line constants and is unrelated to the load impedance, it is also known as natural impedance. Equation (3.75) gives the following value for surge impedance Zn, which is the voltage to current ratio with an impedance dimension:

$$Z_n = \frac{V^2}{I^2} = \frac{L}{C} \tag{76}$$

Inductance $L = \frac{V^2 C}{I^2}$ (77)

Capacitance $C = \frac{I^2 L}{V^2}$ (78)

(a) Propagation Velocity v of Travelling Wave:
To get the velocity of a travelling wave, multiply equations (3.70) and (3.72)

$$VI = ILv \times VCv \tag{79}$$
$$VI = VILCv^2 \tag{80}$$

or

$$v^2 = \frac{1}{LC} \tag{81}$$

or

$$v = \sqrt{\frac{1}{LC}} \tag{82}$$

Where L is the inductance of the line and C is the capacitance of the line, v is the propagation velocity.

(b) Double fault Location on the Transmission Line Based on Travelling Wave.
The most straightforward and reliable traveling wave-based fault finding method is founded on a two-ended principle and has been used in a variety of fault location and protection devices.
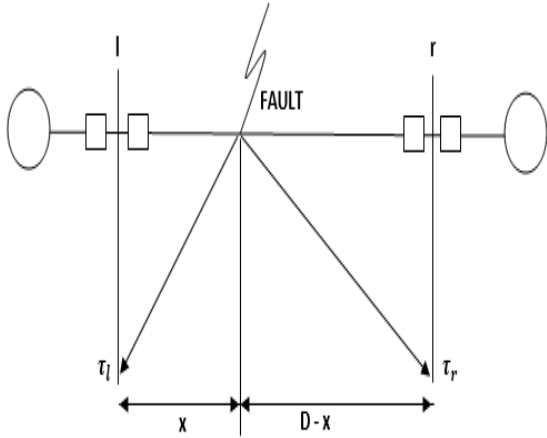
Figure 12: Double Ended Fault Location Based on Time Difference of First Arrival Times

The following formula is used to determine the fault location x after comparing the traveling wave arrival times on both ends of the line;

$$x = \frac{(D + (\tau_l - \tau_r)v)}{2} \qquad (3.83)$$

Where,
D = Total length of the line
τ_l = Departure time at the remote end
τ_r = Arrival time at the local end
v = Propagation velocity

(C) Simulink Modeling of the Traveling Wave Fault Location Equation.
Equation (3.82) is modeled using MATLAB/SIMULINK for the location of any type of fault on the transmission line.

$$\text{Velocity } v = \sqrt{\frac{1}{LC}} \qquad (3.84)$$

But

$$\text{Relay impedance } Z_r = \frac{V^2}{I^2} = \frac{L}{C} \qquad (85)$$

$$\text{Inductance } L = \frac{V^2 C}{I^2} \qquad (86)$$

$$\text{Capacitance } C = \frac{I^2 L}{V^2} \qquad (87)$$

Therefore,

$$\text{velocity } v = \sqrt{\frac{1}{\left(\frac{V^2 C}{I^2}\right) \times \left(\frac{I^2 L}{V^2}\right)}} \qquad (88)$$

The figure 13, 14 and 15 shows the travelling wave propagation process used to simulate the movement of electrical waves along the transmission lines, a typical model used to analyze the fault locations by capturing the transient voltage and current waves generated at the fault point as they propagate in both directions along the line.
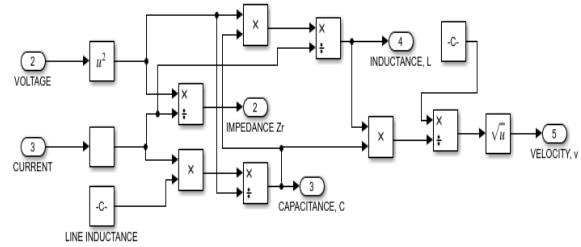
Figure 13: Traveling Wave Propagation Velocity Model
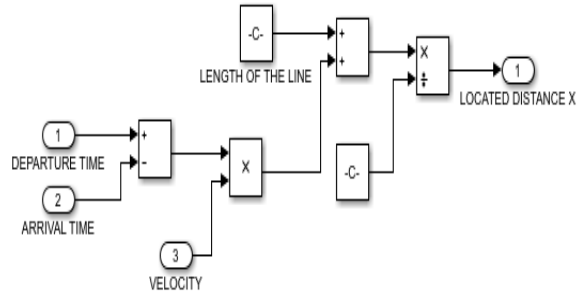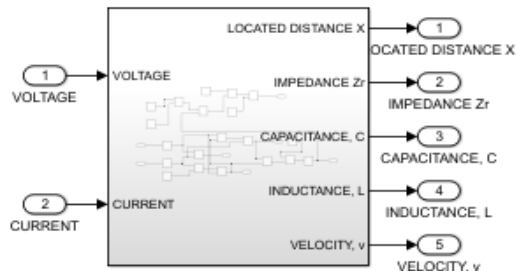

Figure 14: Traveling Wave Fault Location Model

Figure 15: Subsystem of Traveling Wave Fault Location Model

Figure 16 below shows Onitsha – Enugu 330kV, 96km power net work transmission line with travelling wave for fault location.
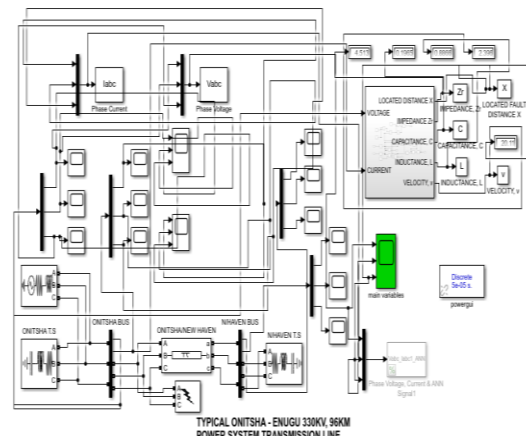

Figure 16: Single Onitsha – Enugu 330KV 96Km Transmission Line

Zones of Protection
The zone on which the fault occurred can be determined using the distance protection zoning system shown below.

Zone 1 setting on the transmission line is 80% of the line distance, Zone 2 setting on the transmission line is 120% of the line distance, and Zone 3 setting on the transmission line is 240% of the total line distance.

Zone 1 is meant to protect the primary line and provide fastest protection because there is no international time delay associated with it. Its operating time can be one cycle.
Zone 1 reach = 0.8 x Total length of the transmission line = 0.8 x 96Km = 76.8Km
Zone 2 reach = 1.2 x Total length of the transmission line = 1.2 x 96Km = 115.2Km
Zone 3 reach = 2.5 x Total length of the transmission line = 2.5 x 96Km = 240Km
The located fault distance is seen on the zone of protection.

Using the MATLAB/SIMULINK modeled equations (75) to (82), we can locate the different symmetrical and unsymmetrical faults using their fault voltage and current parameters.

Figure 17 shows the Onitsha - Enugu 330kV 96km transmission line, viewing the zones of protection.
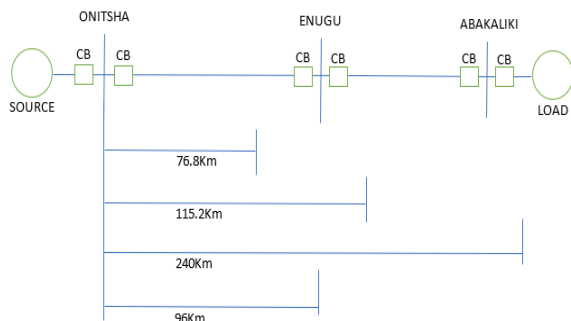
Figure 17: Single Onitsha – Enugu 330KV 96Km Transmission Line

O. Fault Analysis Summary
• Fault current depends on the fault type and the transmission line impedance, and the fault point.
• Sequence network representation simplifies fault analysis.
• System impedance, fault impedance, and pre-fault voltage must all be taken into account in calculations.

P. RESULTS AND ANALYSIS

Regardless of the length of the transmission lines, fault detection is crucial for identifying, tracking, and safeguarding them in the event of a malfunction. The technique focuses on determining the fault's position on the transmission line, its type, and when it happened. Numerous fault kinds, locations, fault resistances, and inception angles are used to evaluate the ANN detector and classifier. Artificial Neural Networks (ANN) for real-time transmission line fault detection and classification can be applied to digital protection of production systems.

The action of each phase's voltage and current forms the basis of this strategy. The presence and type of the fault are indicated by the ANN's outputs. Every test result demonstrates that the fault-suggested detector and classifier can be utilized to accurately and quickly support a new system generation of the protection relay. Because modern power systems are so linked, system stability depends on early failure identification and quick isolation. Transmission line faults must be promptly identified, categorized, and located.

ANNs are utilized for currents as the inputs of neural networks for a variety of reasons. Because Current Transformers (CTs) are always present at each line for measurement and protection purposes, current signals measured at only one end of the line have been used as the inputs to the ANN algorithms. Sometimes, for revenue-related reasons, VTs may not be employed.

Only current signals that are measured at one end of the transmission lines can be utilized to locate and classify faults. Since the neural network uses voltages and currents as inputs, the output of the ANN will produce high-quality results quickly. These voltages and currents are used by the ANN approach to determine the reactive power of the load.

An overview of the use of ANN in transmission line fault detection is provided in this chapter. Since transmission line faults can result in equipment damage, outages, and power system network shutdowns, it is critical to be able to recognize and find them, as discussed in earlier chapters. Therefore, there will be a significant breakdown in the power system's whole networks if transmission line defects go unnoticed.

We need to model transmission lines to ensure that if there is a fault, it can be noticed on time and the ANN can offer reliable data. Three-phase transmission lines have been simulated using Simulink.

The Onitsha-Enugu 330kV, 50 HZ, 96km transmission line is used as a case study to simulate the three-phase power system network model in MATLAB/Simulink software. Figure 3.4 illustrates its components, which include circuit breakers, transmission lines, load, and voltage and current measurements. Powering the load is the primary function of the transmission lines. The generator produces the power supply, which is then sent to the load via the transmission line network.

A circuit breaker is a high-voltage electrical switch designed to protect electrical grids and equipment by automatically disconnecting faulty sections when abnormal conditions occur, such as short circuits, overloads, or system faults.

The load serves as the consumers' feeder, from which the consumers feed, and an ANN can identify certain issues, such as overload current. On the power system, the load can be built as either a radial or a ring feeder; the radial feeder provides a straight-line supply to the consumers, while the ring feeder contains a backup supply.

Earlier systems use a standard method on the transmission lines to detect the fault which takes time to detect the fault and delivers inaccurate findings. The Kirchhoff Voltage and Current Laws on a well-defined transmission line protection model serve as the foundation for conventional algorithms.

The power swing voltage and current is seen by traditional distance relays as a defect and tripping mechanism. Such defective parts would cause serious issues and fuel instability in the power system. Exact results are obtained when Artificial Neural Networks are applied to transmission line failures. Table 3 displays the specifications of the transmission line.

Two three-phase sources make up the three-phase transmission line, which simulates a synchronized power system as seen in Figure 3.4. A PI transmission line component with voltage and current measuring points is part of the transmission line. Furthermore, three-phase loads are dispersed along the transmission line's length. Transmission line phase to ground, phase to phase, and three-phase faults are all simulated by a three-phase fault.

Table 2: Transmission Line Parameters

S/N	LINE PARAMETERS	VALUES
1	Length (km)	96
2	Voltage (kV)	330
3	Positive Sequence Resistance (ohm/km)	0.0114
4	Zero Sequence Resistance (ohm/km)	0.2467
5	Positive Sequence Inductance (ohm/km)	5.684e-4
6	Zero Sequence Inductance (ohm/km)	3.0890e-3
7	Positive Sequence Capacitance (ohm/km)	1.3426e-8
8	Zero Sequence Capacitance (ohm/km)	8.5885e-9

Q. ANN Pre-Processing

Noise and spurious harmonics are commonly superimposed on voltage and current measurements, which can compromise the precision of the ANN's performance. These harmonics are eliminated in practical systems by analog signal filtering, which also reduces undesired signals.

The computation for every phase is carried out and the processing of the simulation data is made simpler by the use of per-unit values.

R. Fault Detection and its Accuracy

Performance Metrics: This discusses metrics such as accuracy, precision, recall, F1-score, and specificity for identifying whether a fault has occurred.

Threshold Sensitivity: It explains how threshold selection impacts the detection accuracy
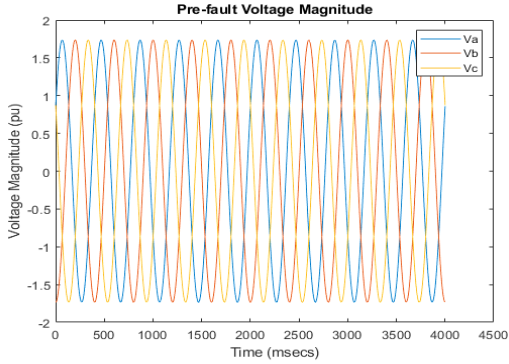
Pre-fault

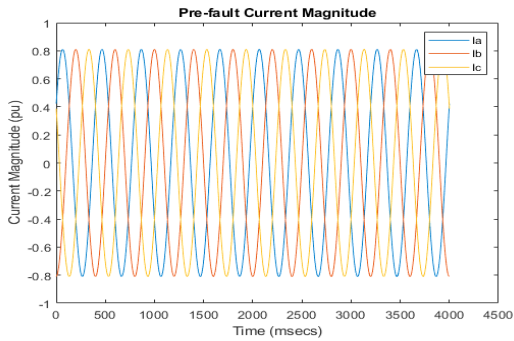Figure 18: Pre-fault Voltage Signal

Figure 19: Pre-fault Current Magnitude

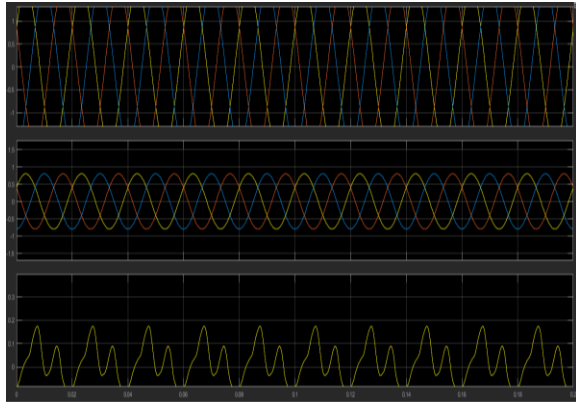ANN Response to Pre-fault V & I Signals

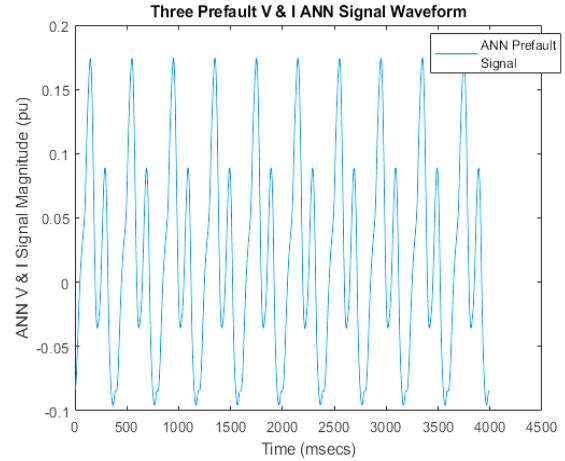Figure 20: ANN Response to Pre-fault V&I Signals

Figure 21: Three – phase Pre-fault V & I ANN Signal Waveform

The Onitsha-Enugu 330kV Power Transmission Line's ANN response plot of pre-fault voltage, current, and their ANN equivalent signal against simulation time prior to fault incidence is shown in Figure 4.4. It demonstrates that the signal magnitudes for the three – phase Pre-fault V & I ANN Signal Waveform is 0.17pu.

R.   Single Line to Ground Fault
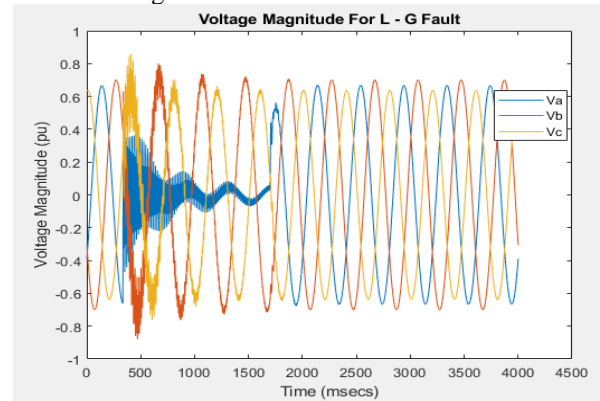
Figure 22: Voltage Magnitude For L – G Fault

Figure 22 illustrates that a fault occurred on one of the lines between 400msecs to 1600msecs, and the voltage (Va) drops to 0.38.
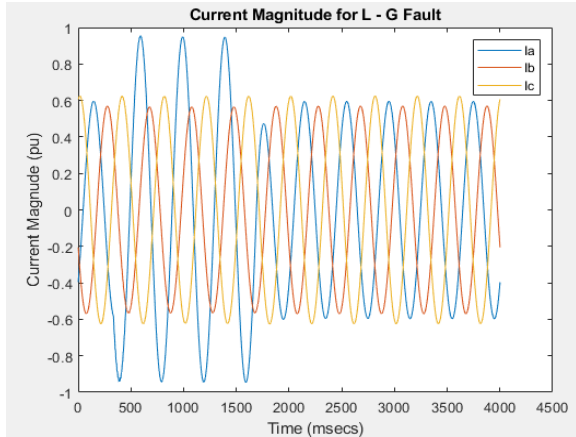
Figure 23: Current Magnitude For L – G Fault

Figure 23 shows that after the voltage (Va) in figure 4.5 reduces to 0.38, the current (Ia) increases.

ANN Response to Fault V&I Signals for L - G

Figure 24 shows the ANN response to voltage and current as a result of the fault that occurred in between the line and ground.
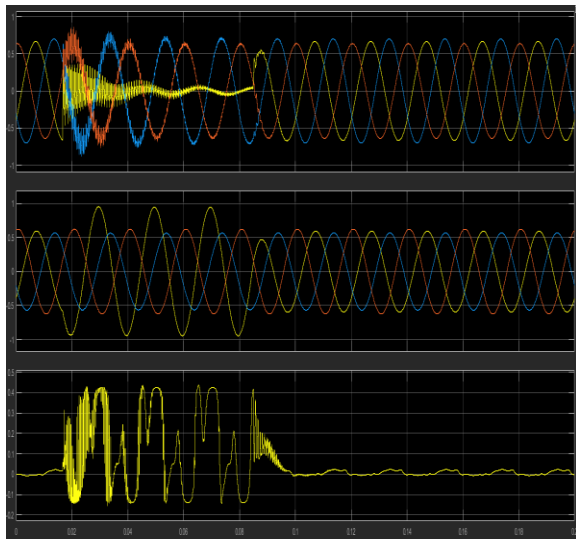

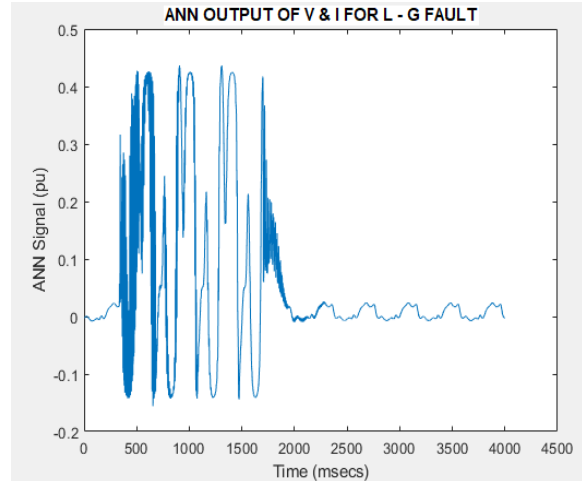Figure 24: ANN Response to Fault V&I Signals for L - G

Figure 25: ANN Output of V&I for L - G Faults

Figure 25 shows the ANN output of the L-G fault voltage and current in figure 4.5 and 4.6.

S. Double Line to Ground Fault
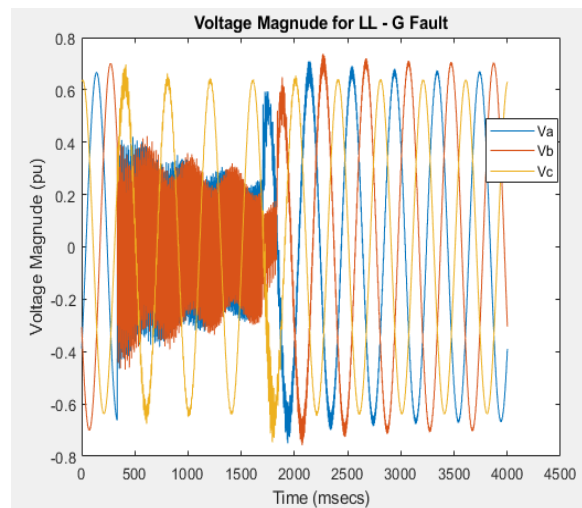
Figure 26: Voltage Magnitude to for LL – G Fault

Figure 26 illustrated a fault occurrence of faults in two of the lines between the period of 400 to 2000msecs, which led to a voltage drop of 0.4pu
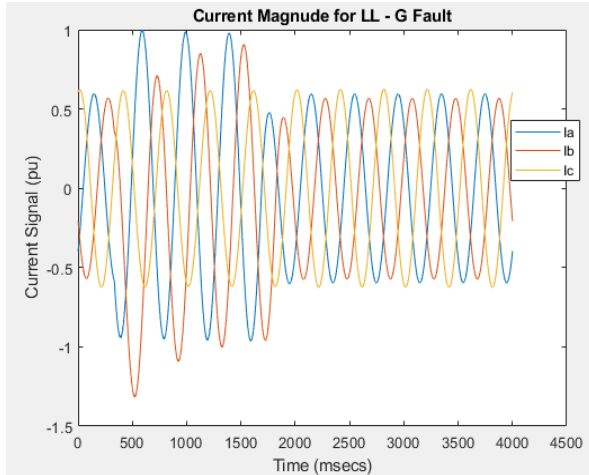
Figure 27: Current Magnitude for LL - G Fault

Figure 27 shows a rise in the current as a result of the fault that occurred in figure 4.9.
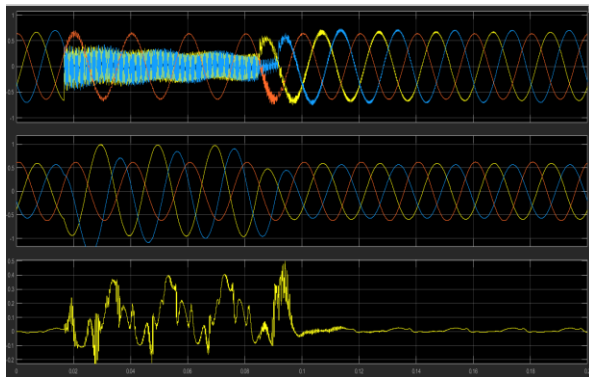
ANN Response to Fault V&I Signals LL - G

Figure 28: ANN Response to Fault V&I Signals LL - G

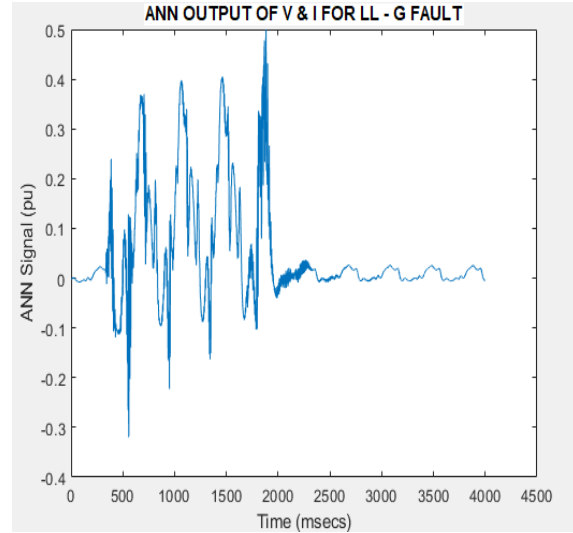Figure 28 shows the ANN response to voltage and current as a result of the fault that occurred onthe lines and ground.

Figure 29: ANN Output of V&I for LL - G Faults

Figure 29 shows the ANN output of the LL-G fault voltage and current in figure 4.9 and 4.10.
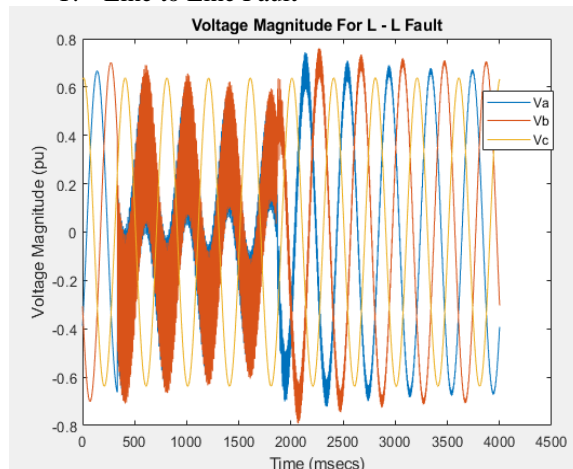
T. Line to Line Fault

Figure 30: Voltage Magnitude to for L – L Fault

Figure 30 illustrates that a fault occurred on one of the lines between 400msecs to 2000msecs, and there was a voltage drop in two of the lines.
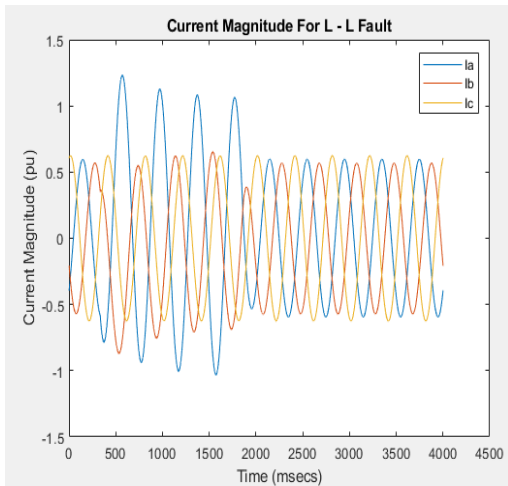
Figure 31: Current Magnitude to for L – L Fault

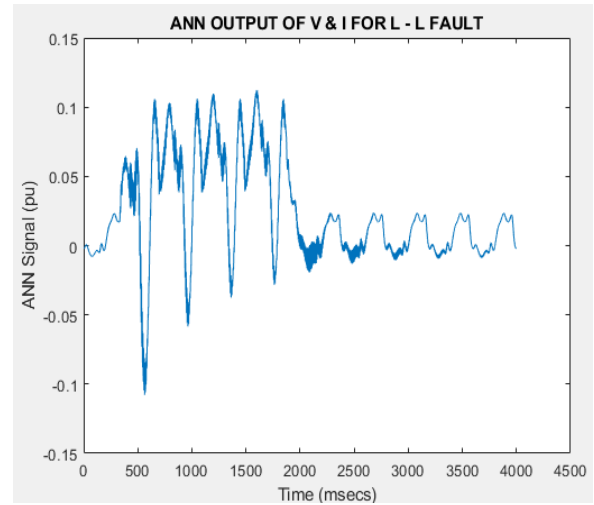Figure 31 shows a rise in the current as a result of the fault that occurred in figure 30
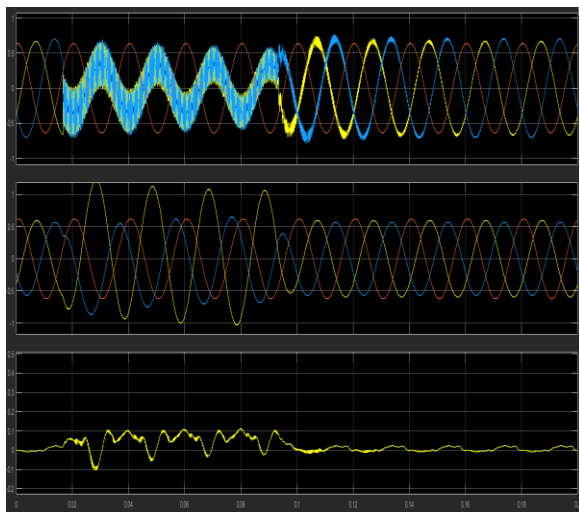

Figure 32: ANN Response to Fault V&I Signals for L – L

Figure 32 shows the ANN response to voltage and current as a result of the fault that occurred on the lines.

Figure 33: ANN Output of V&I for L - L Fault

Figure 33 shows the ANN output of the LL-G fault voltage and current in figure 4.13 and 4.14.

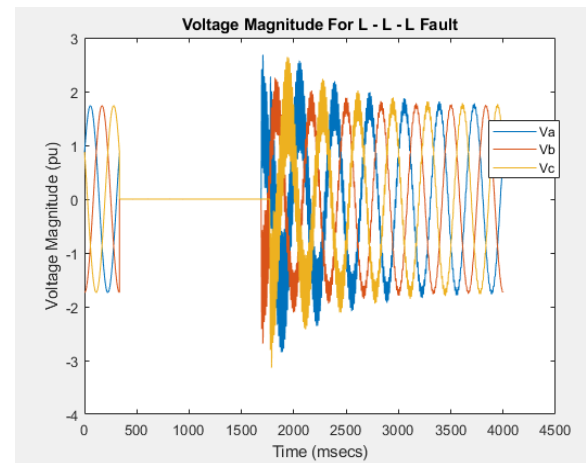U. Three Phase (L – L – L) Fault

Figure 34: Voltage Magnitude For L – L – L Fault

Figure 34 illustrates that a fault occurred on three of the lines between 400msecs to 1600msecs, and Va, Vb and Vc dropped to zero during the period of the fault.
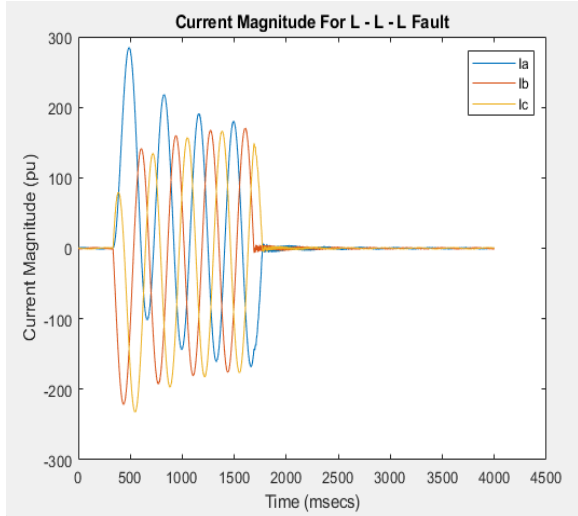
Figure 35: Current Magnitude for L – L – L Fault

Figure 35 shows a rise in the current as a result of the fault that occurred in figure 4.1.
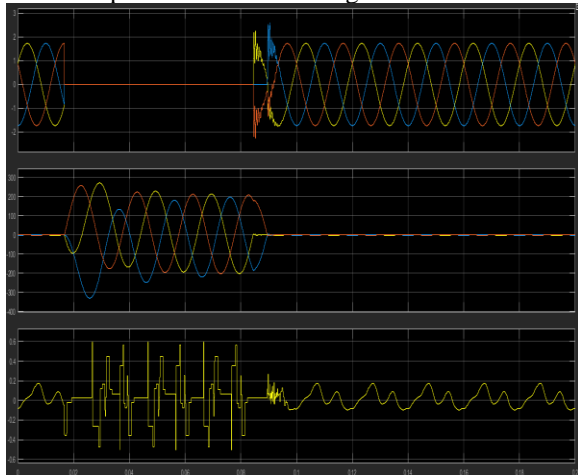
ANN Response to Fault V&I Signals for L – L - L

Figure 36: ANN Response to Fault V&I Signals for L – L - L

Figure 36 shows the ANN response to voltage and current as a result of the fault that occurred on the lines.
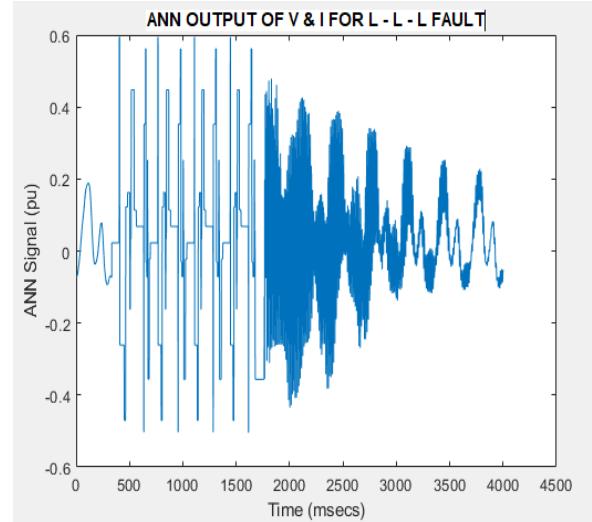

Figure 37: ANN Output of V & I for L – L - L fault

Figure 37 shows the ANN output of the L-L-L fault voltage and current in figure 37 and 38.

V. RESULT SUMMARY FOR THE DIFFERENT TYPES OF FAULTS

Simulation investigations were conducted for various transmission line fault resistances. Pre-fault and three-phase line-line-line (A-B-C) fault types are taken into account.

Figures 4.5 to 4.6, 4.9 to 4.10, 4.13 to 4.14 and 4.17 to 4.18 shows the different types of faults that occurred on the transmission line. It illustrates that when fault occurs in any of the phases, the voltage drastically reduces and in some cases collapses to zero and the current surges.

Figures 4.7 to 4.8, 4.11 to 4. 12, 4.15 to 4.16 and 4.19 to 4.20 shows the ANN voltage and current responses to faults on those lines respectively.

Table 4.2 shows a summary analysis of pre-fault and fault voltage and current and their ANN responses. We can see from table 4.2 at pre-fault, voltage was 1.75 (pu) and current 0.8 (pu). But during faults, there was a voltage drop from 1.75 (pu) to 0.00 and an increase in current from 0.8 to more than 250 (pu), and the ANN response 0.6 which detected that there was a fault. This is acceptable since it supports the findings of electrical standard circuit analysis, which state that anytime a power system malfunction arises, the voltage magnitude will drop and the current will rise.

Table 3: Pre-fault and Fault Data for all the Fault Condition and their ANN Responses

S/N	Va (pu)	Vb (pu)	Vc (pu)	Ia (pu)	Ib (pu)	Ic (pu)	ANN Response (pu)	Fault Type
1.	1.75	1.75	1.75	0.80	0.80	0.80	0.17	Pre-fault
2.	0.38	0.80	0.90	0.90	0.60	0.6	0.43	L-G
3.	0.40	0.40	0.65	1.00	0.90	0.60	0.50	L-L-G
4.	0.50	0.70	0.65	1.3	0.6	0.6	0.13	L-L
5.	0.00	0.00	0.00	280	180	170	0.60	L-L-L

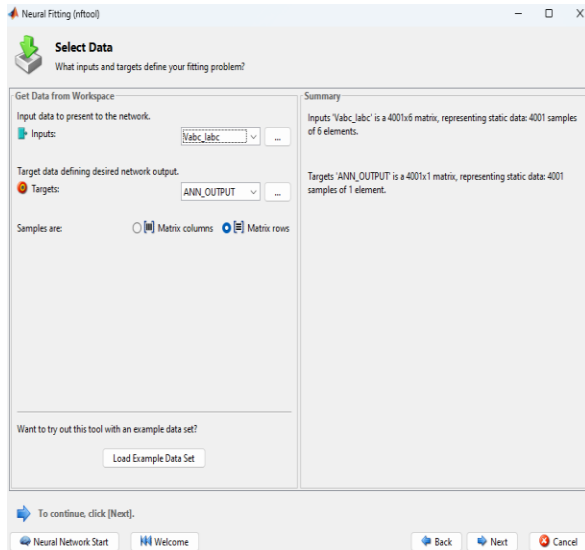W. Training of Data for Detection of Faults

Figure 38: Training of Data for Detection of Faults

Figure 38 show the type of input and output data used for the ANN network architecture for the training fault detection data, while figure 38 shows the number of samples provided for training, validation and testing.
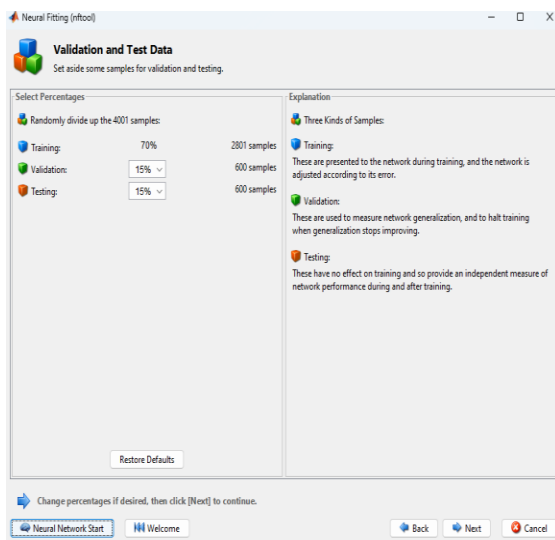

Figure 39: Training Data for validation

X. Valiation of Fault Detection using MATLAB/Simulink Tool

Since the purpose of the section is to check the line's pre-fault condition, the entire 96-kilometer line length is taken into account. The findings indicate that the magnitudes of the three-phase voltages per unit are greater than those of their current counterparts. Electrical circuit theory states that while the line is in a pre-fault state, it is typical for the line voltage magnitude to be higher than the current magnitude.

In order to identify the fault distance on each of the zones when a three-phase fault occurs on the 96km line and to calculate the three-phase fault voltage and current per unit magnitudes, simulation was run on the ten zonal lines.

The chosen ANN for line fault detection was fed the three-phase voltage and current characteristics of each simulated line. The findings display the simulation window procedure, the data training performance, the regression analysis for a suitable fault detection, and the chosen ANN network design for fault detection.

Figure 4.23 below shows an ANN architecture designed to handle 2001 data samples. The ANN architecture was used alongside with the three-phase fault voltages (Va, Vb, and Vc) and currents (Ia, Ib, and Ic) result in Table 4.2, which serves as inputs to the ANN architecture. The ANN architecture has six inputs and one output layer and ten concealed layers. According to its training, its goal is to identify three-phase flaws in Phases A, B, and C. The output depicts a typical fault alert (or trip) since it is taught to respond to any of the fault circumstances that are presented.
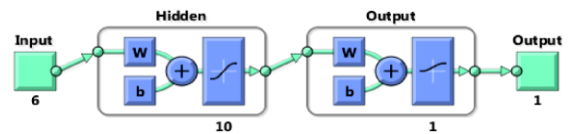
Figure 40: The ANN Selected Architecture or Structure for Fault Detection

In general, figure 40 above was chosen for each of the ten zones with varying line lengths.

A closer look at the input, hidden, and output layers of the developed ANN is provided in figure 40. The ANN Matlab/Simulink Fault Simulator automatically chooses it for transmission line fault identification during fault simulation.

Depending on the complexity of the problem being handled, the neural network's inputs and outputs should have multiple hidden layers, with multiple

neurons in each ANN layer. A neural network with three layers—six neurons in the input layer and one in the output layer—is utilized to detect errors. Based on the Bias Weights (b), the log-sigmoid function assesses the output and suggests the optimal outcomes for the output and hidden layers.

The ANN must be trained in order to obtain the proper magnitude and correlations for the total number of inputs and outputs of the neural network. The size and complexity of the task determine which neural network inputs are used. An artificial neural network's complexity increases with the number of inputs and outputs. As a result, there are many hidden layers. Effective decision-making is made possible by the size of the hidden layers. Three-phase voltages and currents at 50 Hz serve as the basis for the inputs. Both ends of the transmission line were used to measure the three-phase voltages and currents. The ANN output would validate a fault for any of the three phases, and the fault kind was categorized along the transmission line's length.

Y. Fault Classification

Types of Faults: Show how well the ANN performs in accurately identifying various fault types, such as single-phase-to-ground, double-phase, three-phase, etc.

Classification Accuracy: Provides the classification accuracy for each fault type.

Misclassification Analysis: Discusses situations in which faults were misclassified and possible reasons for such errors.

Confusion Matrix: A confusion matrix helps visualize classification performance by showing the number of true positives, false positives, true negatives, and false negatives.
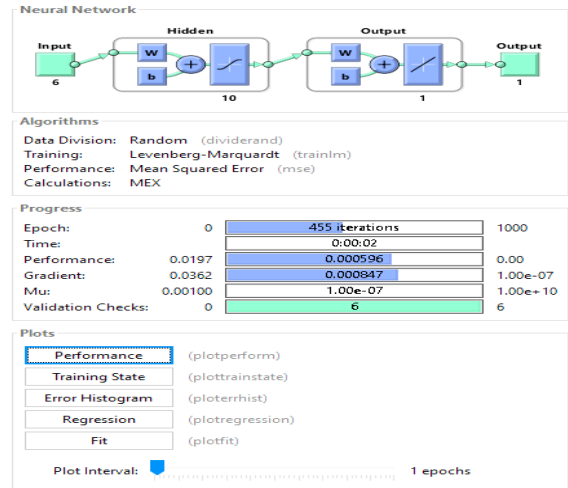
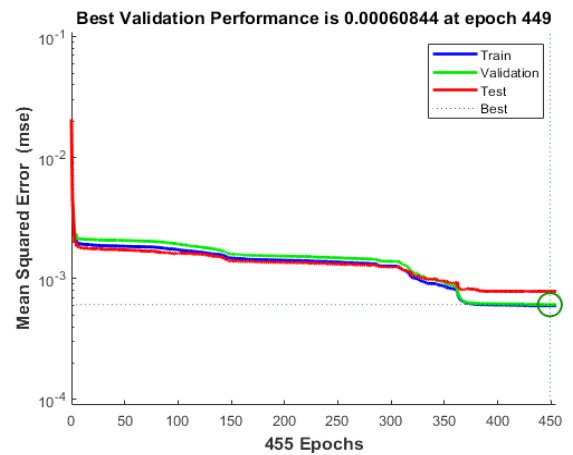Figure 42: ANN Simulation Window Processes

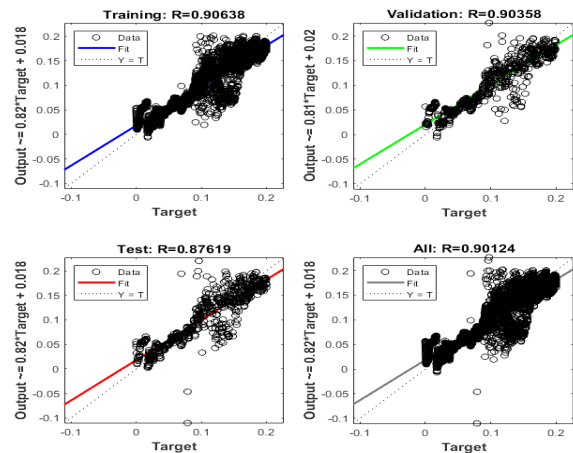Figure 43: Performance for the Training Process of Fault Detection for 96Km

Figure 44: Regression analysis of the ANN for the Fault Detection for 10Km

Figure 44: Shows the number of samples of neurons employed for training, validating, and testing the selected ANN network architecture.

Figure 43 indicates that, at MSE = 6.0844e-4, the training delivers the best training, validation and test outcomes for defect detection.

Figure 44 shows the output versus targets regression curve of the measure of how well the neural network's targets can track the variations in the outputs. The training suggest '0' no correlation at all and '1' a complete correlation. From the result in figure 43 having a coefficient of correlation (R) approximately 1 indicates a good correlation.

Figure 27 and 28 shows a display of another dataset for training testing and validation using an ANN with 6 input, 10 hidden layers and 4 output.
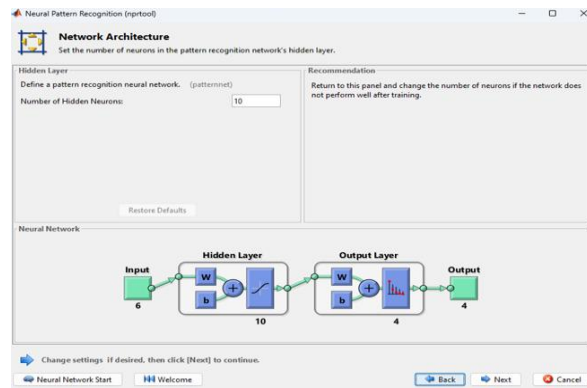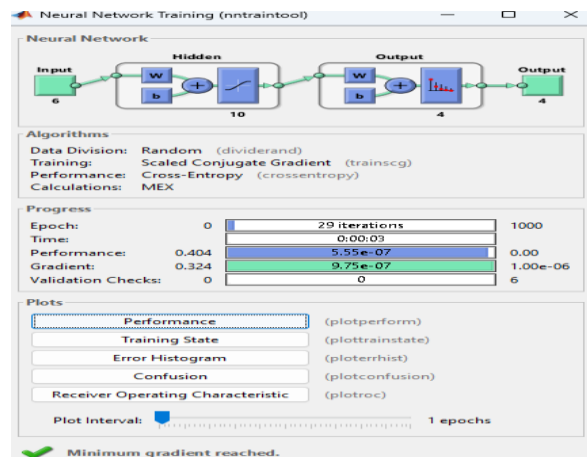

Figure 45: Neural Pattern Recognition
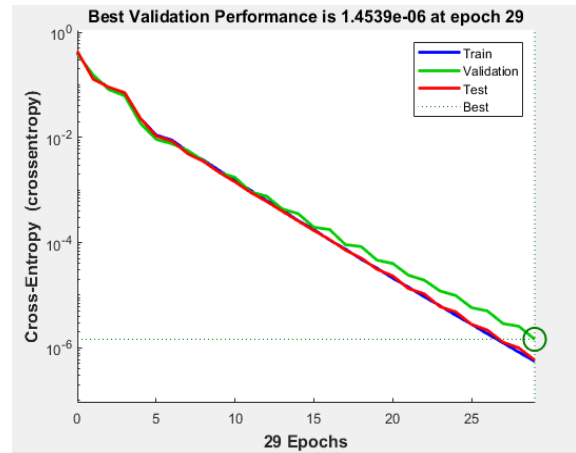

Figure 46: Neural Network Training

Figure 47: Best Validation Performance

The performance graph illustrates the training result of the actions taken place during the trainings process. Figure 47 shows that cross entropy which measures the difference between the predicted probability distribution and the actual, is 1.4539e-06 at 29 epochs. Since the loss of 1.4539e-06 is close to zero, it means the network's predictions are almost perfect.

Figure 48: Neural Network Training Confusion Matrix

Figure 48 above shows the confusion matrices for the various types of errors that occurred for the trained neural network. The confusion matrix for the three phases of training, testing and validation illustrates that the diagonal cells in green colour indicate the number of cases that have been classified correctly by the neural network and the off-diagonal cells which are in pink indicate the number of cases that have been wrongly classified by the ANN. The last cell in white in each of the matrices indicates the total percentage of cases that have been classified correctly in green and the incorrectly in red. It can be seen that the chosen neural network has 100% accuracy in fault classification. Hence the neural network can, with

utmost accuracy, differentiate between the ten possible types of faults on a transmission line.
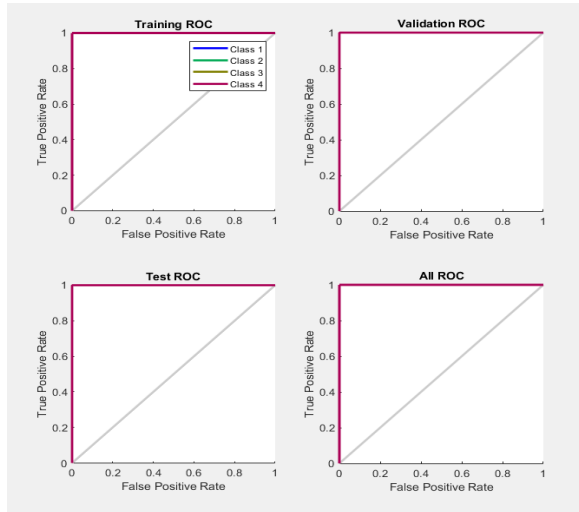

Figure 49: ROC Block

ROC curves provide a comprehensive overview of the performance of a classification model across different threshold values. They plot the true positive rate (TPR) against the false positive rate (FPR) at various threshold settings. This allows for a visual comparison of the trade-offs between sensitivity and specificity.

The Area Under Curve (AUC)summarizes the model's overall ability to classify correctly. It ranges from 0 to 1. Below is a summary of the classification;

- AUC = 1.0 → Perfect classifier.
- AUC ≥ 0.9 → Excellent model.
- AUC ≥ 0.8 → Good model.
- AUC ≥ 0.7 → Fair model

Figure 4.31 represents the receiver operating characteristics (ROC) curves for the confusion matrix in figure 4.31. An area under curve (AUC) of 1.0 was obtained, which makes it a perfect classifier.
Vii
Z. Location of Fault Distance through Zoning
The transmission line between Onitsha and Enugu is 96 kilometers long. The line is set at 10 km for ten different outcomes in this part. Three-phase (A-B-C) fault distances on each of ten kilometers of lines are located using the Traveling Wave MATLAB/Simulink model. The analysis and results are presented and discussed below.

Table 3: Location of Three-Phase Fault (A-B-C) Distance using MATLAB/Simulink Traveling Wave Model

S/N	Line Length (Km)	Line Impedance Zr (Pu)	Located Distance (Km)	Propagation Velocity (M/S)	Wave Departure Time τ_l	Wave Arrival Time τ_r
1	10	0.7672	5.046	0.9892	0.10	0.018
2	20	0.7589	10.50	0.9826	0.10	0.018
3	30	0.7493	15.05	0.9763	0.10	0.018
4	40	0.7409	20.05	0.9708	0.10	0.018
5	50	0.7335	25.40	0.9660	0.10	0.018
6	60	0.7260	30.50	0.9611	0.10	0.018
7	70	0.7184	35.04	0.9560	0.10	0.018
8	80	0.7112	40.84	0.9512	0.10	0.018

By utilizing the MATLAB/Simulink tool to create a traveling wave mathematical model for fault distance location on the Onitsha – Enugu 330KV power system transmission line.

The result indicates that the discovered fault distance increases with increasing line length as the wave signals' propagation velocity and impedance decrease. This results from a shift in the line's topography and the incident point of fault.

As the line length increases, the impedance also increases and the line becomes more vulnerable to a variety of disturbances, including line losses, symmetrical and unsymmetrical faults, wind force effects, etc.

In location of fault distance through zoning, the following terms applies;
i. Fault Location Estimation: Identifying or pinpointing the location of a fault on the transmission line. This is important to maintaining power system reliability.
ii Accuracy of Location: Provides the fault distance estimation mean absolute error (MAE) or root mean square error (RMSE).
iii Impact of Noise: Assess how noise in the system (e.g., due to measurement errors or external disturbances) affects fault location accuracy.
iv Comparison with Standards: Compares ANN's location estimation with conventional methods such as impedance-based or traveling wave methods.

v. Training and Validation
The following terms applies in training and validation of the neural network architecture;
vi Model Convergence: Include plots of training and validation loss to show the convergence of the ANN
vii Validation Performance: Evaluate the extent (how well) of the ANN's performance on unseen validation data.

viii Overfitting or Underfitting: Discuss if there are indications that the model is overfitting or underfitting.

ixTime Performance
The following terms applies in time performance of the neural network architecture;
X Detection Speed: Highlight the real-time capability by reporting the ANN's computing time for fault detection and classification.
Xi Comparison with Real-Time Requirements: Discusses if the detection time satisfies the specifications for a power system operating at 330kv
Xii Robustness to Variation Sensitivity Analysis: The artificial neural network analyzes resilience to changes in fault conditions (ignore noise and irrelevant data), including fault location, fault resistance, and fault inception angle.
Xiii Adaptability: Discuss the ANN's performance under different load conditions and system configurations.

xiv. Visualization
This is visual aids or graphical representation like confusion matrices for classification, the ROC (Receiver Operating Characteristic) curves for detection performance, Plots that display trends under different fault scenarios as well as the estimated location and real locations of faults.
The graphical presentations in plots of all the pre-fault and fault voltages, regression analysis, validation performance, confusion matrix and the Receiver Operating Characteristics (ROC) block has enabled the analysis of results obtained.

xv. Comparative Analysis
Benchmarking:
ANN-based method in comparison to conventional methods;
The ANN-based method has the ability to handle complex data in detection of faults in the transmission lines unlike the conventional methods.
The ANN-based methods can handle non-linear relationships between the inputs and outputs data than the conventional methods
The ANN-based methods has the ability to learn from data and improve accuracy with time than the conventional methods.
It is equipped with real -time fault diagnosis than the conventional methods such the impedance based method.
The combination of the neural network and the travelling wave significantly enhanced the fault detection and location accuracy in the transmission lines by the high-speed and precise nature of the travelling wave method and the Artificial Neural Network learning capability to improve robustness and adaptability.

xvi. Conclusion
Neural networks have been used in this thesis as a viable and efficient technique for identifying, classifying, and locating transmission line faults. The techniques used, make use of neural networks with inputs that are the sum of the wavelet decomposed fault voltage and current values for each of the three phases. This work has considered a number of potential fault types, including line-ground, line-line, double line-ground, and three phase faults, and distin ANNs have been implemented for each of these fault types.

Every neural network used in this thesis is a back-propagation neural network architecture that uses the Scaled Conjugate Gradient algorithm or the Levenberg-Marquardt algorithm.

Artificial neural networks have been successfully used to develop a fault location scheme for the transmission line system, from the line fault detection stage to the fault location stage.

The results of the simulation demonstrated that the suggested neural network had performed satisfactorily. As further demonstrated, the size of the ANN (the number of hidden layers and the number of neurons per hidden layer) varies continuously based on the neural network's application and the size of the training data set. This work has emphasized the significance of selecting an appropriate ANN configuration to achieve optimal network performance. The line parameters employed in this work are 330kv for voltage, 96km for length, conductor resistance of 0.02Ω/Km, inductance of 1.2mH/km, capacitance of $0.01\mu f/Km$ and 50Hz frequency to sample the voltage and current waveforms.

REFERENCES

[1] Aggarwal, R. K., Johns, A. T., Song, Y. H., Dunn, R. W., and Fitton, D. S. (March, 1994). Neural-network based adaptive single-pole auto-reclosure technique for EHV transmission systems. IEE Proc. on Generation, Transmission and Distribution, vol. 14, no. 2, pp. 155–160.

[2] Abdulwahid, A. H. (2019). A new concept of an intelligent protection system based on a discrete wavelet transform and neural network method for smart grids. International conference of the

IEEE Nigeria computer chapter retrieved from https://doi.org/10.1109/nigeriacomputconf4597 4.2019.8949618, on (June 2024)

[3] Ajay, S.S., Akshit, S. and Ankit, N. (2017). Fault Analysis on Three Phase Transmission Lines and its Detection. International Journal of Advance Research and Innovation. Volume 5 Issue 2. 229-233 ISSN 2347 – 3258.

[4] Anazia, E. A., Anionovo, U. E. and Ogboh V. C.(2020). Time – Frequency Analysis Technique for Fault Investigation on Power System Transmission Lines. International Journal of Engineering Inventions, 9(6), 18-25.

[5] Aneke, J.I., and Ezechukeu, O.A. (2018). Fault Identification and Location in Power Transmission Lines Using Multi - Resolutional Analysis (MRA) and Pattern Recognition.https://phd-dissertations.unizik.edu.ng/repos/81172439950_133122801518.pdf.

[6] Aravind, K., Linu, B., Juhina, A., Saritha, M., Joel O.B., Priya S., and Viji C., (2015). Fault Detection and Location in Transmission Line using Pole Climbing Robort''. International Journal of Engineering Science & Research Technology. ISSN: 2277-9655.

[7] Arboleda, E.R., Delfino, J.C. and Sarmiento, J.L. (2024). Machine learning advances in transmission line fault detection: A literature review International Journal of Science and Research Archive. Retrieved from Article DOI: https://doi.org/10.30574/ijsra.2024.12.1.1150on (May 2024).

[8] Anyalebechi, A.E., Nwangugu, E.C., and Ogboh, V. C. (2019). Fault Detection on Power System Transmission Line Using Artificial Neural Network (A Comparative Case Study of Onitsha–Awka–Enugu Transmission Line. American Journal of Engineering Research (AJER) 2019, 8(4), 32-57

[9] Eriksson, L., Saha, M. M, Rockefeller, G. D. (2015).An accurate fault locator with compensation for apparent reactance in the fault resistance resulting from remote-end feed. IEEE Trans on PAS 104(2), pp. 424-436.

[10] Ezechukwu, O.A, Ogboh, V.C, and Madueme, T. C. (2019) Analysis of Fault Detection Algorithm for Power System Transmission Lines Using DFT And FFT''. Ire Journals | Volume 3 Issue | ISSN: 2456-8880 Ire 1701668 Iconic Research and Engineering Journals 142.

[11] Ezechukwu, O.A., Onuegbu, J. and Okwudili, O. E. (2019). Artificial Neural Network Method for Fault detection on Transmission Line. International Journal of Engineering Inventions E-ISSN: 2278-7461, P-ISSN: 2319-6491 Volume 8, Issue 1 [January 2019] PP: 47-56 www.Ijeijournal.Com

[12] Dash, P., Panda, G. and Samantaray, S. (2006). Fault classification and location using HS-transform and radial basis function neural network. Electric. Power Syst. Res. 76, 897–905.

[13] Gupta, S. K. (2009). Power System Engineering. January 2009''. 4232/1, Ansari Road, Dariyaganj, Delhi-110002 ISBN: 978-81-88114-91-7.

[14] Gupta, P.D. and Mahanty, R. (2007). A fuzzy logic based fault classification approach using current samples only. Electric. Power Syst. Res. 77, 501–507.

[15] Haque, M. T., and Kashtiban, A. M. (2005). Application of Neural Networks in Power Systems; A Review. Proceedings of world academy of Science, Engineering and Technology Vol. 6 ISSN 1307-6884.

[16] Hasabe, R. P., and Vaidya A. P. (2014). Detection and classification of faults on 220 KV transmission line using wavelet transform and neural network. International Journal of Smart Grid and Clean Energy, vol. 3, no. 3.

[17] Haykin, S. (1994). Neural Networks, A Comprehensive Foundation. Macmillan College Publishing Company.

[18] Jamil, M., Sharma, S.K. and Singh, R. (2015). Fault detection and classification in electrical power transmission system using artificial neural network. https://doi.org/10.1186/s40064-015-1080-x

[19] Kim, K.H. and Park J.K. (1993). Application of hierarchical neural networks to fault diagnosis of power systems", International journal of

electrical power and energy systems Vol.15, No.2, p65-70.

[20] Kasztenny B., Rosolowski E., Saha M. and Hillstrom B. (2015). A self-organizing fuzzy logic based protective relay – an application to power transformer protection. IEEE Transactions on Power Delivery, Vol. 12, No. 3, pp. 1119-27.

[21] Kezunovic, M. (1997). A survey of neural net applications to protective relaying and fault analysis. International Journal of Engineering Intelligent Systems for Electronics, Engineering and Communications 5(4), pp. 185-192.

[22] Kumar, M., Nelish. S., Singh, R., Wallender W. W., and Pruitt, W. O.(2002). Estimating Evapotranspiration using Artificial Neural Network. Journal of irrigation and Drainage Engineering, 128, 224-233.

[23] Liu, Y., and Yao, X. (1996). A Population based Learning Algorithm which Learns both Architectures and Weights of Neural Networks", Proceeding of ICYCs95 Workshop on Soft Computing Vol.3 No.1, Allerton Press Inc. New York.

[24] Liu, X., Wang, Z., Tao, X., Xu, D., Zhang, D. and Zhang, H. (2018). Detection of power line insulator defects using aerial images analyzed with convolutional neural networks. IEEE transactions on systems, man, and cybernetics systems. Retrieved from https://doi.org/10.1109/tsmc.2018.2871750, on (May 2024).

[25] Mamta Patel, and Patel, R. N. (2012). Fault Detection and Classification on a Transmission Line using Wavelet Multi Resolution Analysis and Neural Network. International Journal of Computer Applications (0975 – 8887) Volume 47– No.22.

[26] Ranaweera, D.K. (1994). Comparison of neural network models for fault diagnosis of power systems. Electric Power Systems Research, Vol.29, No.2, p99-104.

[27] Ryan, H M., Tindle, J. and Wong, K.C. (1996). Power system fault prediction using artificial neural networks. In: Progress in Neural Information Processing. SET (Amari, S. -I.;Xu, L.; Chan, L. -W.; King, I. and Leung, K. -S. eds.),

Springer, London, UK, pp.1181–1186.URLhttps://oro.open.ac.uk/17762

[28] Saad, A., Sidra, A., Syeda, F.N., Qaiser, A., and Kulsoom, U. (2023). Fault detection and power diagnosis in power system using AI: A review received August 15, 2023; Revised November 20, 2023; Accepted March 28, 2024.

[29] Saha, M. M., Izykowski, J., Rosolowski, E. (2010). Fault Location on Power Networks. Springer publications.

[30] Sachdev, M.S., Sidhu, T.S., and Singh, H. (1995). Design, implementation and testing of an artificial neural network based fault direction discriminator for protecting transmission lines. IEEE Trans. On Power Delivery, vol. 10, no., pp 697-706.

[31] Saadat, H. (1999). Power System Analysis. New York. The McGraw-Hill Companies, Inc.

[32] Tayeb, E.B. (2013). Fault detection in power system using Artificial Neutral Network. American Journal of Engineering Research (AJER) e-ISSN : 2320-0847 p-ISSN : 2320-0936 Volume-02, Issue-06, pp-69-75 www.ajer.org